Erythrocyte scaffolding protein p55/MPP1 functions as an essential regulator of neutrophil polarity

Brendan J. Quinn[a], Emily J. Welch[a], Anthony C. Kim[a], Mary A. Lokuta[b,1], Anna Huttenlocher[b], Anwar A. Khan[a], Shafi M. Kuchay[a], and Athar H. Chishti[a,2]

[a]Department of Pharmacology, University of Illinois College of Medicine, Chicago, IL 60612; and [b]Departments of Pediatrics and Pharmacology, University of Wisconsin, Madison, WI 53706

Edited by Henry R. Bourne, University of California, San Francisco, CA, and approved September 16, 2009 (received for review June 23, 2009)

As mediators of innate immunity, neutrophils respond to chemoattractants by adopting a highly polarized morphology. Efficient chemotaxis requires the formation of one prominent pseudopod at the cell front characterized by actin polymerization, while local inhibition suppresses the formation of rear and lateral protrusions. This asymmetric control of signaling pathways is required for directional migration along a chemotactic gradient. Here, we identify the MAGUK protein p55/MPP1 as a mediator of the frontness signal required for neutrophil polarization. We developed a p55 knockout ($p55^{-/-}$) mouse model, and demonstrate that $p55^{-/-}$ neutrophils form multiple transient pseudopods upon chemotactic stimulation, and do not migrate efficiently in vitro. Upon agonist stimulation, p55 is rapidly recruited to the leading edge of neutrophils in mice and humans. Total F-actin polymerization, along with Rac1 and RhoA activation, appear to be normal in $p55^{-/-}$ neutrophils. Importantly, phosphorylation of Akt is significantly decreased in $p55^{-/-}$ neutrophils upon chemotactic stimulation. The activity of immunoprecipitated phosphatidylinositol 3-kinase γ (PI3Kγ), responsible for chemoattractant-induced synthesis of PIP_3 and Akt phosphorylation, is unperturbed in $p55^{-/-}$ neutrophils. Although the total amount of PIP_3 is normal in $p55^{-/-}$ neutrophils, PIP_3 is diffusely localized and forms punctate aggregates in activated $p55^{-/-}$ neutrophils, as compared to its accumulation at the leading edge membrane in the wild type neutrophils. Together, these results show that p55 is required for neutrophil polarization by regulating Akt phosphorylation through a mechanism that is independent of PI3Kγ activity.

Akt | erythrocyte p55 | MPP1 | MAGUK

In response to chemotactic stimuli, neutrophils adopt a highly polarized morphology that coordinates their directed cell migration toward sites of injury and inflammation (1). Neutrophil polarity is characterized by an asymmetric distribution of signals to distinct intracellular locations, a process critical for directional sensing and chemotaxis (2). Polarity requires directional sensing of external cues by cell surface receptors, triggering a reorganization of the cortical cytoskeleton. At the leading edge of neutrophils, the process is regulated by receptor-mediated activation of G_i, which results in activation of the small GTPase, Rac, and accumulation of the membrane signaling lipid, phosphatidylinositol-3,4,5-triphosphate (PIP_3). PIP_3, Rac, and F-actin together participate in a positive-feedback loop that leads to the formation of a single robust pseudopod, even when cells are exposed to a uniform concentration of formyl-Met-Leu-Phe, fMLP (3–6). Neutrophils treated with selective inhibitors of PI3Kγ respond to fMLP by forming multiple transient pseudopods laterally, as well as at the leading edge rather than a single persistent pseudopod at the leading edge (3). These neutrophils exhibit quantitatively normal amounts of F-actin, further supporting the hypothesis that PIP_3 acts to amplify the signal locally, thus confining Rac activation and F-actin polymerization to a distinct region (4–6).

The G protein-dependent class I_B PI3K, p110γ, is the isoform responsible for the chemoattractant-induced PIP_3 production in neutrophils (7, 8). Stimulation of neutrophils with fMLP enhances the activity of I_B PI3K, p110γ but not the class I_A subunits p85/p110 in immunoprecipitates (7). Neutrophils treated with the PI3Kγ inhibitors PIK-90 or -93, which inhibit the production of PIP_3, respond to chemoattractants by forming multiple pseudopods, whereas neutrophils treated with the class I_A PI3K inhibitors polarize normally (3). Furthermore, neutrophils from p110γ knockout mice exhibit both defective chemotaxis in vitro and reduced accumulation in the peritoneal cavity in response to inflammatory stimuli in vivo (8–11). This evidence indicates that stimulation of PI3Kγ causes a rapid increase in the accumulation of PIP_3, which in turn drives pseudopod formation, thus maintaining neutrophil polarity. However, a major challenge is the identification of the components that regulate localized accumulation of PIP_3 at the leading edge of activated cells.

P55, also called the Membrane Palmitoylated Protein 1 (MPP1), is a prototypical member of a family of signaling proteins termed MAGUKs (membrane associated guanylate kinase homologues). MAGUKs share a number of protein domains including the PDZ domain, a single src-homology-3 (SH3) motif, and a domain homologous to guanylate kinases (GUK) (12, 13). P55 was originally identified as a scaffolding protein in erythrocytes stabilizing the actin cytoskeleton to the plasma membrane by forming a tripartite complex with protein 4.1R and glycophorin C (14, 15). Although p55 is ubiquitously expressed, its function in nonerythroid cells remains poorly understood. The p55 gene is composed of 12 exons spanning approximately 28 kb in the q28 region of the human X chromosome (16). The murine homologue of p55 is located in the syntenic region of the mouse X chromosome (17). Using conventional gene targeting and deletion techniques, we generated a mouse model systemically lacking p55. Here, we present evidence that p55 regulates neutrophil polarity, and functions as a positive upstream effector of Akt phosphorylation. These unexpected findings unveil a role for p55 in neutrophil polarity with functional implications for both autoinflammatory diseases and infections.

Results

Targeted Deletion of Mouse MPP1 Gene. Erythrocyte p55/MPP1 is the founding member of a subgroup of MAGUKs (12, 13). The p55-like MAGUKs currently include seven members in the human genome, and each member is characterized by the presence of PDZ, SH3, and GUK domains (Fig. 1*A*). In addition to these three core domains, some p55-like MAGUKs also contain the L7B domain in the N terminus, the D5 domain that binds to cytoskeletal protein 4.1, a tyrosine phosphorylation (TP) motif, and a very C-terminal sequence of unknown function (12, 18). Although

Author contributions: A.H. and A.H.C. designed research; B.J.Q., E.J.W., M.A.L., A.H., A.A.K., and S.M.K. performed research; E.J.W. and A.A.K. contributed new reagents/analytic tools; B.J.Q., E.J.W., M.A.L., A.H., A.A.K., S.M.K., and A.H.C. analyzed data; and B.J.Q. and A.H.C. wrote the paper.

The authors declare no conflict of interest.

This article is a PNAS Direct Submission.

[1]Present address: Stratatech Corporation, Suite 169, 505 South Rosa Road, Madison, WI 53719.

[2]To whom correspondence should be addressed. E-mail: chishti@uic.edu.

This article contains supporting information online at www.pnas.org/cgi/content/full/0906761106/DCSupplemental.

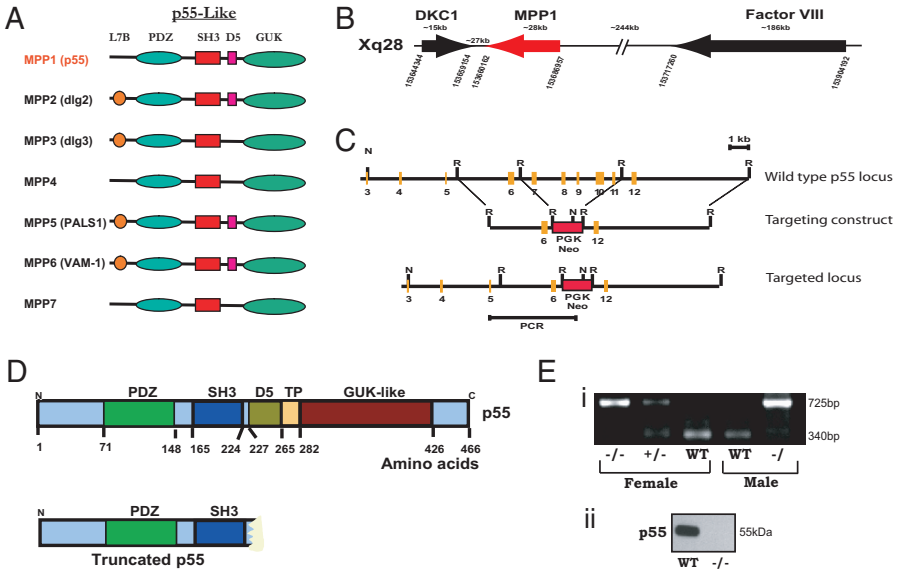

Fig. 1. Generation of p55$^{-/-}$ mice. (*A*) Domain structure of the p55-like MAGUKs. Seven family members (MPP1-MPP7) have been identified in mammals. (*B*) Location of the p55/MPP1 gene in the q28 region of the human and mouse X chromosome. Both MPP1 and factor VIII genes are transcribed in the same orientation while the gene for X-linked dyskerotosis congenita (dyskerin/DKC1) lies tail to tail with MPP1. (*C* and *D*) Gene targeting construct for the deletion of p55/MPP1 gene. The C-terminal half of p55 was deleted including the D5, TP, and GUK domains encoded by exons 7–11. (*E*) Confirmation of the genotype by PCR of tail DNA, and Western blotting of p55 in the erythrocyte ghosts.

detailed biochemical characterization of several p55-like MAGUKs has been performed, the in vivo function of these proteins remains unknown as no mouse models of the gene deficiency have been reported for any of the seven members. Using standard gene targeting approaches, we systemically deleted the C-terminal half of p55 that includes exons 7–11 (Fig. 1 *B–E*). This finding was confirmed at the protein level by Western blotting of erythrocytes where p55 is abundantly expressed (Fig. 1*E*). We used several antibodies generated against p55 to firmly establish the protein null phenotype: (a) Rabbit polyclonal antibody against native erythrocyte p55; (b) Rabbit polyclonal antibody against the N-terminal peptide, PEMP1 (EVRKVRLIQFEKVTEE); (c) Rabbit polyclonal antibody against the D5 domain peptide (EAPSCSPFGKKKKYK); and (d) Mouse monoclonal antibody raised against the GUK domain of p55. Affinity-purified antibodies failed to detect any trace of the full length as well as the N-terminal truncated peptide of p55 in erythrocytes and other tissues confirming the generation of p55 null mouse model (Fig. S1).

Phenotype Characterization of p55$^{-/-}$ Mice. The p55$^{-/-}$ mice were born at normal Mendelian ratios but their litter size was consistently small (3–5 pups). Initial pathology report indicated that the liver, heart, kidney, adrenal gland, spleen, pancreas, lung, cerebrum, cerebellum, and medulla oblongata of p55$^{-/-}$ mice were within normal limits. Initial analysis of peripheral blood obtained from three adult animals indicated no major differences in hematologic indices including white blood cell number. The morphology of erythrocytes from p55$^{-/-}$ mice appears to be normal; however, detailed analysis will be required to assess the role of p55 in the linkage of protein 4.1R with glycophorin C. Some of these studies are currently underway in our laboratory.

The MPP1 gene located on human Xq28 was originally mapped within a CpG island 30 kb centromeric to the factor factor VIII gene (19). Both MPP1 and factor VIII genes are transcribed in the same orientation from telomere to centromere (20). Interestingly, the gene for X-linked dyskerotosis congenita (dyskerin/DKC) lies tail to tail with MPP1 gene on Xq28 (20). Patients with dyskeratosis congenita display increased susceptibility to cancer particularly affecting the progenitors in the skin and bone marrow (21). Due to the close proximity of MPP1 and DKC genes, we examined whether our deletion of the MPP1 gene may have affected the expression of the DKC gene. Polyclonal antibodies against the N-terminal (residues 74–88) and the C-terminal (residues 382–396) peptides of mouse dyskerin did not show any alteration of dyskerin protein expression in the p55$^{-/-}$ tissues. In addition, we examined p55 expression in the erythrocytes of a hypomorphic *Dkc1* mutant mouse model that recapitulates some features of human dyskeratosis congenita (22). Again, no difference in the level of p55 was

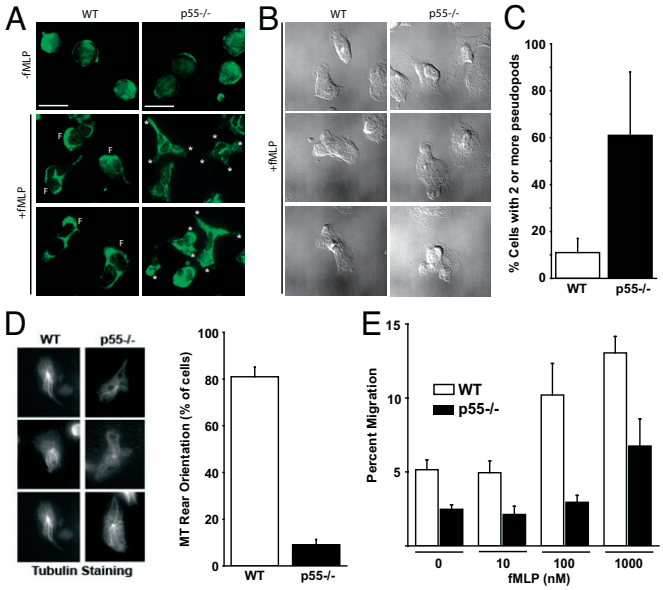

Fig. 2. Defective polarity and migration of p55$^{-/-}$ neutrophils. (*A* and *B*) Morphology of WT and p55$^{-/-}$ neutrophils. Mouse BM marrow neutrophils were plated onto fibronectin and stained with FITC-conjugated Phalloidin. WT neutrophils form one prominent leading edge rich in F-actin (*F*) whereas the p55$^{-/-}$ neutrophils extend multiple pseudopods (asterisks). (*C*) Neutrophils with two or more pseudopod extensions were counted in a field of 400 cells. (*D*) β-tubulin staining was performed to quantify the polarity defect. Upon stimulation, WT neutrophils orient their microtubule network from the centrosome toward the rear of the cell. P55$^{-/-}$ neutrophils exhibit radiating microtubules in a pinwheel pattern, as quantified in the graph. (*E*) Transwell migration of WT and p55$^{-/-}$ neutrophils. After 30 min, cells that migrated into the lower chamber containing fMLP were counted and represented as percent of the total cells added to the upper chamber. The p55 loss caused a reduction in the number of migrating neutrophils recovered from the lower chamber, particularly at higher concentrations of fMLP (100 nM and 1 μM). Each bar represents the mean value $\pm$ 2 SEM of three separate experiments.

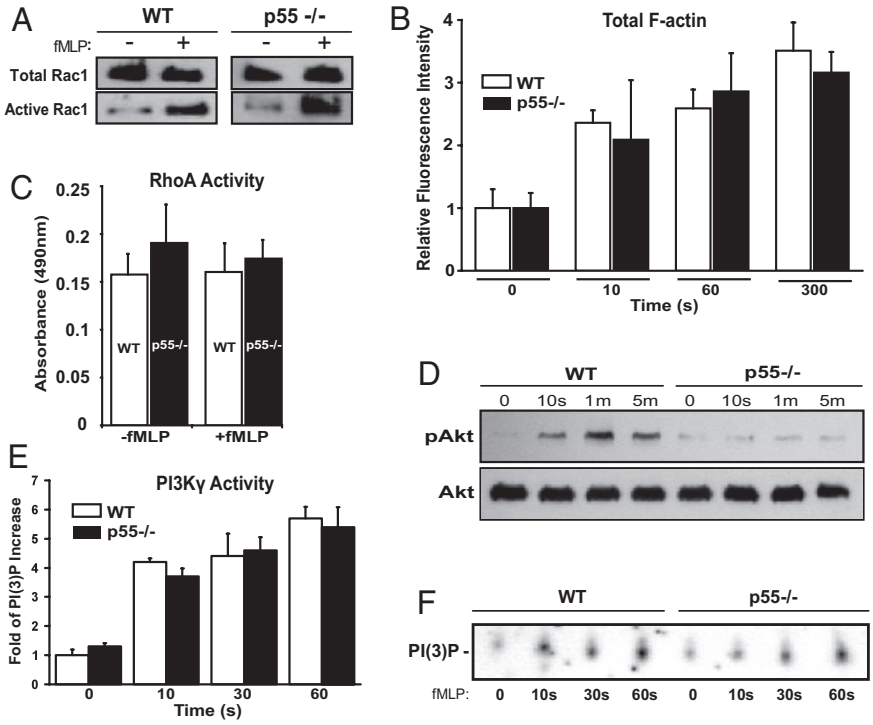

Fig. 3. Biochemical characterization of p55$^{-/-}$ neutrophils. (*A*) Rac1 activation. Neutrophils were stimulated with 1 μM of fMLP and lysate was analyzed by the pull-down assay. Western blotting was performed using an anti-Rac1 monoclonal antibody. No difference was observed in the total or active Rac1 between WT and p55$^{-/-}$ neutrophils. Blot is representative of three separate experiments. (*B*) Total F-actin polymerization. Neutrophils were stimulated with 1 μM fMLP, fixed in cold paraformaldehyde, permeabilized, and incubated for 1 h with 0.2 μM FITC-conjugated Phalloidin. Cells were washed and analyzed by flow cytometry. Bars represent the mean fluorescence intensity relative to time 0 (no fMLP). No difference was observed in the polymerized F-actin between WT and p55$^{-/-}$ neutrophils (graph represents three experiments). (*C*) RhoA activation. RhoA activity was measured using an ELISA-based kit (Cytoskeleton Inc). RhoA activation was comparable between WT and p55$^{-/-}$ neutrophils (graph represents three experiments). (*D*) Phosphorylation of Akt. WT and p55$^{-/-}$ neutrophils were stimulated with 1 μM fMLP and lysates were analyzed by Western blotting using a polyclonal antibody against Akt. This antibody detects phosphorylated threonine-308. Total Akt blotting was used to confirm equal loading in each lane. Blot is representative of four separate experiments. (*E*) Activity of PI3Kγ. PI3Kγ was immunoprecipitated from WT and p55$^{-/-}$ neutrophils, and its activity was measured by in vitro production of PI(3)P. The intensity of the PI(3)P spots were normalized to time 0, and the data shown represents three separate experiments. (*F*) A representative autoradiograph of one PI3Kγ activity assay.

observed by Western blotting. These observations suggest that the expression of DKC gene is not affected in the p55$^{-/-}$ mice. However, we cannot rule out the possibility that the absence of p55 may affect specific functions of dyskerin protein in some tissues.

Disrupted Polarity and Inefficient Chemotaxis in p55$^{-/-}$ Neutrophils. During our previous studies on the characterization of erythrocyte p55, we developed a highly specific monoclonal antibody directed against the GUK domain (23). This antibody detected robust expression of p55 in both human and mouse neutrophils (Fig. S1). The serendipitous finding led us to investigate the role of p55 in mouse neutrophils. First, the morphology of bone marrow neutrophils was visualized upon plating onto fibronectin-coated coverslips. Neutrophils were stimulated with a uniform concentration of 100 nM fMLP for 5 min, fixed, permeabilized, and stained for F-actin. Neutrophils lacking p55 respond to fMLP by forming multiple lateral pseudopods instead of the single clearly-defined leading or trailing edge pseudopod as observed in WT neutrophils (Fig. 2*A* and *B*). Greater than 60% of p55$^{-/-}$ neutrophils extended more than one pseudopod (Fig. 2*C*). To further quantify the loss of polarity, WT and p55$^{-/-}$ neutrophils were immunostained for β-tubulin and the percentage of cells with a rear orientation of the microtubule network were counted (Fig. 2*D*). Roughly 80% of WT neutrophils orient their microtubules toward the back of the cell upon stimulation compared to only approximately 11% of p55$^{-/-}$ neutrophils. The loss of polarity in p55$^{-/-}$ neutrophils predicted a defect in cell migration in response to chemoattractants. To test this hypothesis, in vitro transwell assays were performed. Loss of p55 expression resulted in a reduced number of neutrophils migrating through the filter into the lower chamber of a transwell device, especially at higher concentrations of fMLP (Fig. 2*E*). Furthermore, time-lapse video microscopy showed that p55$^{-/-}$ neutrophils eventually migrate toward a micropipette point-source of chemoattractant, but take circuitous routes to reach it (Movies S1 and S2). This abnormal migratory behavior appears to be a direct consequence of defective polarization and the inability of p55$^{-/-}$ neutrophils to form a single leading edge pseudopod that orients itself toward the chemotactic gradient. Fig. S1*F* shows that p55$^{-/-}$ neutrophils also form uropod-like structures enriched in phospho-ERM.

F-Actin Polymerization and GTPase Activation in p55$^{-/-}$ Neutrophils. Using a specific monoclonal antibody against p55, we established the presence of p55 in human neutrophils by Western blotting (Fig. S1*A*). Next, p55 was localized in both resting and stimulated human neutrophils by immunofluorescence microscopy. In resting neutrophils, p55 is uniformly distributed around the cell periphery (Fig. S1*B*). Upon treatment with chemoattractant, the majority of p55 translocated to the leading edge and co-localized with the F-actin (Fig. S1*B*). This observation suggests that p55, like other MAGUKs, may be involved in the trafficking of critical membrane components, and participates in the formation of protein complexes at the neutrophil leading edge. Biochemical analysis was performed on WT and p55$^{-/-}$ neutrophils to investigate the activation of well-known regulators of the polarization pathway. Total F-actin polymerization was quantified in neutrophils by incubating cells with FITC-Phalloidin and analyzing relative fluorescence by flow cytometry. There was no significant difference in the total amount of F-actin polymerization between WT and p55$^{-/-}$ neutrophils after stimulation with fMLP at various time points (Fig. 3*B*). This observation is consistent with the immunofluorescence images showing the presence of F-actin staining in the multiple pseudopod extensions of p55$^{-/-}$ neutrophils (Fig. 2*A*).

Next, we investigated the activation of the small GTPases, Rac1 and RhoA, which function as critical components of neutrophil gradient sensing and polarization (3, 4). Using a well-established GST-PBD based pull-down assay (24), the total amount of active Rac1 was measured in WT and p55$^{-/-}$ neutrophils stimulated with fMLP. There was no significant difference in Rac1 activation (Fig. 3*A*). To measure active RhoA, a more sensitive chemiluminescence-based G-LISA was used. Again, the activation of RhoA was comparable between WT and p55$^{-/-}$ neutrophils (Fig. 3*C*).

Phosphorylation of Akt Is Reduced in p55$^{-/-}$ Neutrophils. The presence of multiple pseudopods in p55$^{-/-}$ neutrophils resembles

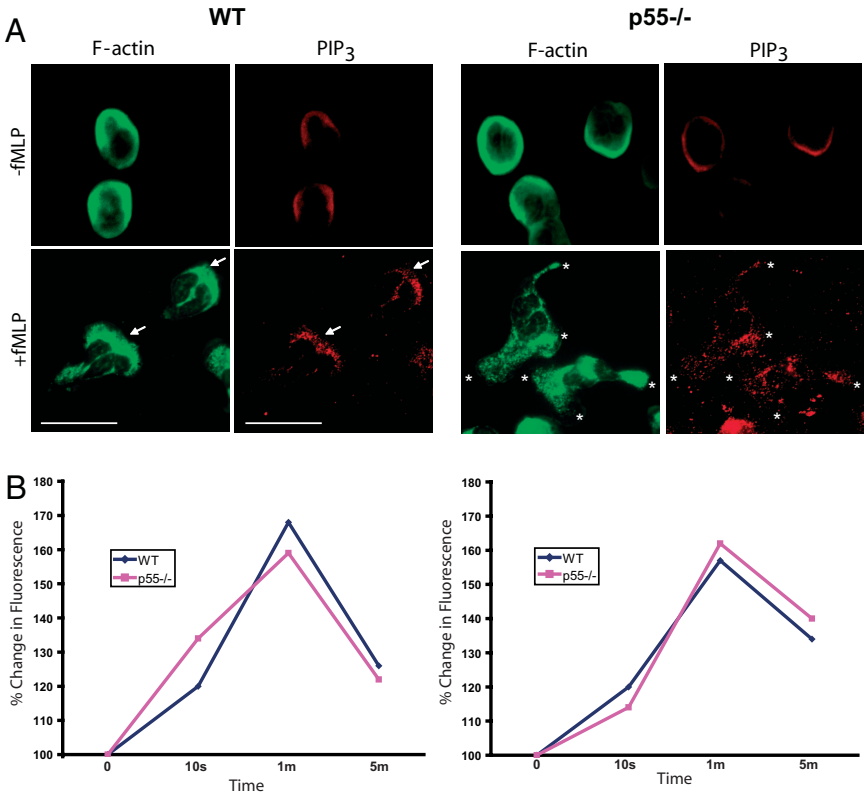

Fig. 4. PIP_3 localization and its content. (*A*) Localization of PIP_3 in $p55^{-/-}$ neutrophils. A monoclonal anti-PIP3 antibody was used to stain PIP_3 in resting and activated WT and $p55^{-/-}$ neutrophils. In resting cells, there was a faint signal of PIP_3 around the peripheral membrane. Upon stimulation with fMLP, WT neutrophils polarized by accumulating PIP_3 toward the leading edge membrane marked by F-actin staining. Upon stimulation, $p55^{-/-}$ neutrophils formed extensions but PIP_3 is diffusely localized throughout the cytosol. (*B*) Neutrophils were incubated with anti-PIP_3 antibody and FACS analysis was performed to measure total PIP_3 levels after fMLP stimulation. No difference in total PIP_3 was observed between WT and $p55^{-/-}$ neutrophils. Two independent experiments are shown.

neutrophils treated with specific inhibitors of PI3Kγ (3). Therefore, we examined the phosphorylation of Akt as a downstream indicator of PI3K activity and/or PIP_3 accumulation in $p55^{-/-}$ neutrophils (Fig. 3*D*). WT and $p55^{-/-}$ neutrophils were stimulated with fMLP, and lysates were analyzed by Western blotting using a polyclonal antibody that specifically recognizes Akt that is phosphorylated at threonine 308 ($pAKT^{T308}$). In WT neutrophils, there was an immediate phosphorylation of Akt that peaked at 1 min and gradually decreased by approximately 50% within 5 min (Fig. 3*D*). This phosphorylation of Akt corresponds to rapid activation of PI3Kγ and the production and accumulation of PIP_3. In contrast, Akt phosphorylation was significantly reduced in $p55^{-/-}$ neutrophils at each time point after fMLP stimulation (Fig. 3*D*). The total amount of Akt protein was comparable between WT and $p55^{-/-}$ neutrophils in four independent experiments. These results suggest that p55 mediates cell polarity by regulating the PI3Kγ-PIP_3 pathway that is critical for the stability and maintenance of the leading edge pseudopod in neutrophils.

Status of PI3Kγ Activity in $p55^{-/-}$ Neutrophils. Neutrophils lacking PI3Kγ show reduced Akt phosphorylation after fMLP stimulation as compared to WT neutrophils (8). Furthermore, neutrophils treated with the PI3Kγ inhibitors show multiple lateral pseudopods upon stimulation (3), a feature that is similar to activated $p55^{-/-}$ neutrophils (Fig. 2*A*). Therefore, we examined whether the reduced Akt phosphorylation in $p55^{-/-}$ neutrophils resulted from alterations of PI3Kγ. PI3Kγ was immunoprecipitated from WT and $p55^{-/-}$ neutrophils and its lipid kinase activity was measured (Fig. 3*E*). Immunoprecipitated PI3Kγ was incubated with phosphatidylinositol and [^{32}]ATP, the lipid products were separated by thin layer chromatography, and the formation of radiolabeled phosphatidylinositol 3-phosphate, PI(3)P, was observed (Fig. 3*F*). The production of PI(3)P, which reflects the enzymatic activity of PI3Kγ, was similar in WT and $p55^{-/-}$ neutrophils (Fig. 3*E*). These results suggest that p55 does not directly affect the activity of PI3Kγ, but may be involved in the localization of either PI3Kγ or PIP_3. Alternatively, p55 may participate in a signaling pathway that regulates Akt phosphorylation in neutrophils in a previously unrecognized manner. Fig. S1*E* shows a comprehensive Western blot of the canonical signaling components of the PI3K-Akt pathway. In $p55^{-/-}$ neutrophils, only the phosphorylation of Akt (at both T308 and S473) is affected.

Status of PIP_3 in $p55^{-/-}$ Neutrophils. Our current hypothesis is that p55 regulates PIP_3 localization at specific membrane sites of polarized neutrophils. To analyze PIP_3 we used a monoclonal anti-PIP_3 antibody (Invitrogen). To validate the specificity of this antibody, we measured the PIP_3 immunofluorescence signal in neutrophils treated with the PI3Kγ inhibitor PIK-90, and observed a significant reduction in PIP_3 staining (shown in Fig. S1*G*). In resting WT and $p55^{-/-}$ neutrophils, PIP_3 staining was uniformly localized around the cell periphery (Fig. 4*A*). Upon activation of WT neutrophils, PIP_3 translocates to the leading edge as defined by F-actin staining. In activated $p55^{-/-}$ neutrophils PIP_3 does not consolidate to one region, but rather forms punctate aggregates at various sites of F-actin polymerization (Fig. 4*A*). In addition, we measured total PIP_3 content in the resting and activated WT and $p55^{-/-}$ neutrophils (fixed and permeabilized) using the anti-PIP_3 monoclonal antibody and TRITC-conjugated anti-mouse IgM. The PIP_3 content was measured by measuring the relative fluorescence intensity by flow cytometry (Fig. 4*B*). No significant difference was observed in the total PIP_3 content of WT and $p55^{-/-}$ neutrophils at four different time points of activation, corresponding to the data shown in the PI3Kγ assay (Fig. 3*E*). Thus, the production of PIP_3 is not altered under these conditions. Since PIP_3 is diffusely localized in activated $p55^{-/-}$ neutrophils, our results suggest that p55 may regulate PIP_3 trafficking or its tethering to the leading edge plasma membrane. In the absence of p55, PIP_3 is still produced at quantitatively normal levels, but forms punctate aggregates throughout activated $p55^{-/-}$ neutrophils, thus inhibiting Akt phosphorylation at specific membrane sites.

Discussion

The original cloning and characterization of p55/MPP1 as a heavily palmitoylated peripheral membrane protein in human erythrocytes led to its current designation as one of the founding members of the MAGUK family of scaffolding proteins (13, 18). In mature erythrocytes, p55 forms a ternary complex with protein 4.1R and glycophorin C with implications in the regulation of cell shape and membrane stability (25). MAGUKs, including the *Drosophila* Dlg tumor suppressor, function as regulators of cell polarity (26). Recent findings have shown that p55 forms a complex with whirlin and regulates cell polarity during hair cell development (27). Mutations in the whirlin gene cause deafness and Usher syndrome, and p55 also interacts with MPP5 to link the Usher protein network with the Crumbs protein complex in the retina (28). These observations suggest a role for p55 in the regulation of the apico-basal Crumbs polarity complex and actin polymerization in both ear and retina. Despite this improved biochemical understanding, the biological function of p55 remains unexplored as no animal models of p55 deficiency exist.

In this manuscript, we report the generation and characterization of a mouse model with systemic p55 null phenotype. The p55 knockout model provides evidence for the essential role of p55 in neutrophil polarity. In contrast to WT neutrophils, which polarize to form a defined leading and trailing edge upon stimulation with chemoattractants, the $p55^{-/-}$ neutrophils form multiple pseudopods in all directions (Fig. 2 *A* and *B*). Consequently, they lack a prominent leading edge resulting in impaired chemotaxis (Fig. 2*E*). Because $p55^{-/-}$ neutrophils extend pseudopods in random directions, they fail to chemotax efficiently. Time-lapse video microscopy shows that $p55^{-/-}$ neutrophils eventually reach a pipette tip dispensing chemoattractant, but take circuitous paths in achieving their final destination (Movies S1 and S2). Neutrophils are the first responders to infection; and thus their delayed migration could compromise the effectiveness of the immune response. A detailed future study will determine the precise in vivo function of p55 in inflammation and infections using a large number of age-matched $p55^{-/-}$ mice with different genetic backgrounds.

To investigate the biochemical basis of p55 function in neutrophil polarity, we examined its role in the reorganization of the actin cytoskeleton in lieu of its known interactions with protein 4.1R at the actin-spectrin junction in the erythrocyte membrane (14). Moreover, it is well established that the regulation of F-actin polymerization by small Rho GTPases serves as a critical determinant of the frontness signal in neutrophils (1). Despite the colocalization of p55 with F-actin at the front end of activated WT neutrophils (Fig. S1*A*), polymerization of F-actin and activation of Rac1 and RhoA appear to be unaltered in $p55^{-/-}$ neutrophils (Fig. 3). This finding was not surprising as $p55^{-/-}$ neutrophils are still able to assemble and extend pseudopods, albeit in random directions. The formation of multiple protrusions in $p55^{-/-}$ neutrophils suggests that their polarity defect originates either from the defective stabilization of the leading edge pseudopod and/or the inability to inhibit the formation of pseudopods elsewhere. It appears that this spatial separation of polarity signals is compromised in $p55^{-/-}$ neutrophils.

Using the $p55^{-/-}$ model, we provide evidence that p55 regulates a signaling pathway that lies upstream of Akt phosphorylation in neutrophils. In WT neutrophils, Akt phosphorylation occurs within 10 s following agonist stimulation peaking at around 1 min. Upon stimulation with fMLP, the $p55^{-/-}$ neutrophils show a marked decrease in Akt phosphorylation at all time points (Fig. 3*D*). This observation suggests that p55 either directly regulates neutrophil PI3Kγ activity or indirectly influences PIP_3-dependent processes that are upstream regulators of Akt phosphorylation.

The morphology of $p55^{-/-}$ neutrophils resembles human neutrophils treated with specific inhibitors of PI3Kγ (3). To investigate the possibility that p55 may regulate PI3Kγ activity, we immunoprecipitated PI3Kγ and measured its activity (Fig. 3 *E* and *F*). PI3Kγ activity was comparable between the WT and $p55^{-/-}$ neutrophils, suggesting that p55 functions either downstream of PI3Kγ or regulates Akt phosphorylation through an alternative pathway. To examine this issue further, we measured total PIP_3 produced in the neutrophils after chemotactic stimulation. No difference was observed in the amount of PIP_3 in WT and $p55^{-/-}$ neutrophils, a feature consistent with the PI3Kγ activity assay. In resting WT and $p55^{-/-}$ neutrophils, the PIP_3 staining is uniformly localized around the cell periphery (Fig. 4*A*). Upon activation of WT neutrophils, the PIP_3 translocated and accumulated at the leading edge as defined by F-actin staining. Interestingly, the PIP_3 is diffusely localized and forms punctate aggregates in activated $p55^{-/-}$ neutrophils (Fig. 4*A*). PIP_3 appears to aggregate at sites of F-actin polymerization, where the cell may be trying to form pseudopods. Since PIP_3 consolidation at the leading edge is essential during polarization, we surmise that the punctate localization of PIP_3 in activated $p55^{-/-}$ neutrophils contributes to the morphologic instability of these cells (Fig. 5). Future studies will determine if p55 can directly interact with or influence PIP_3 trafficking and localization.

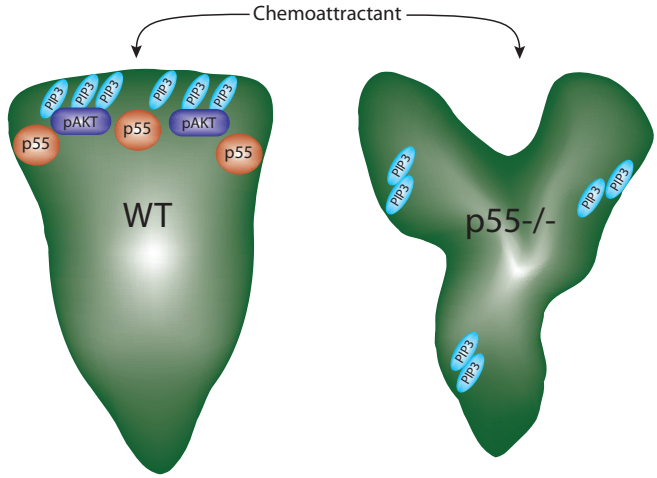

Fig. 5. PIP_3 accumulation and Akt activation in neutrophil polarity. In the model, activated WT neutrophils polarize to form one leading-edge pseudpod enriched in PIP_3 and p55. This accumulation of PIP_3 promotes phosphorylation of Akt. In $p55^{-/-}$ neutrophils, chemoattractants induce the extension of multiple pseudpods in various directions. PIP_3 aggregates in various locations coinciding with F-actin polymerization, rather than accumulating at one leading edge. PIP_3 has emerged as a critical mediator of pseudopod stability during neutrophil polarization. Because total PIP_3 production is unchanged in the absence of p55, we hypothesize that the polarity and Akt-phosphorylation defects are due to abnormal trafficking or accumulation of PIP_3 at the front of the cell.

In summary, we identified a role of p55, a major palmitoylated erythrocyte membrane protein, in the regulation of neutrophil polarity. This finding lends further credence to the emerging paradigm that MAGUKs function as critical regulators of cell polarity. The p55 null mouse model will help to expedite the elucidation of the precise mechanism of p55-dependent signaling pathways that amplify the cellular polarization process in neutrophils and in many other cells. Whether the known Xq28-linked immune deficiency disorders and myeloid abnormalities are influenced by p55/MPP1 will now be testable in the near future.

Materials and Methods

Construction of p55 Targeting Construct. Primer pair M1/M3 (M1: 5′ CAT CTC AAC AGA GGA GAT GAC; M3: 5′ CAC TGT TTC AAA TTT GGT GCC) derived from exon 10 of the murine p55 cDNA, was used to screen a Mouse ES-129 P1 genomic library

(Genome Systems) (29). P1 clone #3975, determined to contain the murine p55 gene by dot blot analysis, was EcoRI digested and shotgun subcloned into the vector pGEM-4Z. A 3.5 kb EcoRI fragment containing exon 6 and flanking introns was subcloned into the EcoRI site of the targeting plasmid pPGK, upstream of the neomycin (neo) cassette. A 8 kb EcoRI fragment containing exon 12 and flanking introns was subcloned into a modified pCR2.1 vector (Invitrogen) allowing the excision of this fragment using the enzymes NotI and SacII. The 8 kb arm was then subcloned into a NotI-SacII site downstream of the neo cassette. The final targeting construct resulted in the deletion of a 6.5 kb EcoRI fragment containing exons 7–11 and the insertion of a neo cassette. Exons 7–11 encode the protein 4.1-binding domain (D5) and the guanylate kinase-like (GUK) domain of p55 (Fig. 1*D*).

Embryonic Stem Cell Transfection and Blastocyst Injection. The targeting construct (≈50 μg) was linearized at the unique SacII site and electroporated into the R1 embryonic stem (ES) cell line using standard techniques (30). The G418-resistant clones were screened for homologous recombination by PCR analysis. Primers derived from the exon 5 and the neo cassette (including a nested pair), were used to amplify a junction fragment (≈4 kb) from the correctly targeted allele. A single ES clone (2H7), positive by PCR analysis, was expanded for blastocyst injection and genomic DNA isolation. NcoI-digested genomic DNAs from 2H7, 2H11, and C129/Sv were hybridized to an external 2.5-kb probe that spanned exons 4 and 5, to confirm correct homologous recombination. Mutant allele is distinguished by the presence of a 9 kb band, while the wild-type allele is identified as a 10 kb band. A single band is detected in the 2H7 lane due to the fact that R1 ES cells are derived from male embryos and thus have only one X chromosome. To generate p55 null mice, 2H7-ES cells were injected into C57BL/6J blastocysts followed by implantation into pseudo pregnant mice. The resulting male chimeras were bred with C57BL/6J females to produce hemizygous males (−/), and heterozygous females (+/−), which were subsequently mated to generate homozygous females (−/−). A combination of Southern blotting and PCR analysis was used for genotyping of mice. The antibodies used in Western analysis included a monoclonal antibody raised against the GUK domain of p55 and an affinity-purified antibody generated against an N-terminal peptide sequence encoded by exon 2 of p55.

Mice. p55$^{-/-}$ mice were back-crossed against C57BL/6J mice for six generations before being used for experiments. Mice were housed in a barrier facility located in the Biological Resources Laboratory at the University of Illinois College of Medicine, Chicago, and all experiments were performed in accordance with the guidelines of the Animal Care Committee.

Isolation of Mouse Neutrophils. Bone marrow (BM) cells were isolated from femurs and tibias of adult mice and layered onto a NycoPrep (Axis-Shield)/72% Percoll (Sigma) gradient. After centrifugation for 30 min at 2,600 rpm, cells at the interface were collected into HBSS filled tubes and washed. Eighty-five to ninety percent of the cells are mature neutrophils as determined by Wright Giemsa staining and Gr-1$^+$ FACS analysis. Human primary neutrophils were isolated from the whole blood of healthy donors by discontinuous 55/72% Percoll gradient centrifugation. For human cells, approximately 95% of those collected at the interface are mature neutrophils.

Chemotaxis Assay. Mouse BM neutrophils (4×10^5) in warm RPMI were added to the upper chamber of a 3-μm pore size filter (BD Biosciences) inserted into a 24-well plate. The lower chambers were filled with varying concentrations of fMLP in RPMI, and the plate was incubated for 30 min at 37 °C. After incubation, the filters were removed and the medium in the lower chamber was collected. Cell counts were obtained from a hemacytometer.

GTPase Pull-Down Assays. Assays to measure active Rac1 were carried out as described previously (24). Briefly, a GST fusion protein of the p21-binding domain of PAK (PBD) was expressed in bacteria and coupled to glutathione-Sepharose beads. The GST-PBD-coupled beads were added to neutrophil lysates and incubated for 45 min at 4 °C. Beads were washed three times with 1× lysis buffer and boiled in Laemmli sample buffer. SDS/PAGE and Western blotting were performed as described above, using a monoclonal anti-Rac1 antibody (BD Biosciences). To measure RhoA activity, lysates were analyzed using a RhoA G-LISA kit according to the manufacturer's instructions (Cytoskeleton Inc).

Antibodies and Reagents, Actin Polymerization Assay, Immunofluorescence, Lysate Preparation and Immunoblotting, PI3Kγ Activity Assay, Measurement of Total PIP$_3$ and Video Microscopy. For detailed methods, please see *SI Text*.

ACKNOWLEDGMENTS. We thank Dr. John O'Bryan (University of Illinois, Chicago) for sharing the GST-PBD construct, technical advice, and many helpful discussions; Betsy Mitchell, Dr. Christopher Southgate, Gary Sclar, Jennifer Wu, and Dr. Pil-Soo Seo for help with the microinjection experiments and other technical assistance; Dr. Aida Metzenberg (California State University, Northridge) for sharing anti-peptide antibodies against p55; Dr. Philip Mason (Washington University, St. Louis) for antibodies against dyskerin; Dr. Davide Ruggero (University of California, San Francisco) for providing us blood samples from hypomorphic Dkc1 mutant mice; Dr. Kevan Shokat (University of California, San Francisco) for generously providing PIK-90; Drs John Quigley, Toshihiko Hanada, Kaori Yamada, Jingsong Xu, Karen Snapp, Chinnaswamy Tiruppathi, and Richard Ye for critical comments and discussions during the course of these studies; and Deanna Rybak, Adam Wieschhaus, and Mori Mohseni of our laboratory for careful reading and editing of the manuscript. Gene targeting experiments by Anthony Kim were performed at St. Elizabeth's Medical Center, Boston, MA. This work was supported by the National Institutes of Health grants HL60755, CA 94414, and the Department of Defense Neurofibromatosis Research Program Career Development Award NF020087 from the Department of Defense (to A.H.C.).

1. Servant G, et al. (2000) Polarization of chemoattractant receptor signaling during neutrophil chemotaxis. *Science* 287:1037–1040.
2. Bagorda A, Parent CA (2008) Eukaryotic chemotaxis at a glance. *J Cell Sci* 121:2621–2624.
3. Van Keymeulen A, et al. (2006) To stabilize neutrophil polarity, PIP3 and Cdc42 augment RhoA activity at the back as well as signals at the front. *J Cell Biol* 174:437–445.
4. Weiner OD, et al. (2002) A PtdInsP(3)- and Rho GTPase-mediated positive feedback loop regulates neutrophil polarity. *Nat Cell Biol* 4:509–513.
5. Wang F, et al. (2002) Lipid products of PI(3)Ks maintain persistent cell polarity and directed motility in neutrophils. *Nat Cell Biol* 4:513–518.
6. Sasaki AT, Chun C, Takeda K, Firtel RA (2004) Localized Ras signaling at the leading edge regulates PI3K, cell polarity, and directional cell movement. *J Cell Biol* 167:505–518.
7. Naccache PH, et al. (2000) Stimulation of human neutrophils by chemotactic factors is associated with the activation of phosphatidylinositol 3-kinase gamma. *J Biol Chem* 275:23636–23641.
8. Hirsch E, et al. (2000) Central role for G protein-coupled phosphoinositide 3-kinase gamma in inflammation. *Science* 287:1049–1053.
9. Hannigan M, et al. (2002) Neutrophils lacking phosphoinositide 3-kinase gamma show loss of directionality during N-formyl-Met-Leu-Phe-induced chemotaxis. *Proc Natl Acad Sci USA* 99:3603–3608.
10. Ferrandi C, et al. (2007) Phosphoinositide 3-kinase gamma inhibition plays a crucial role in early steps of inflammation by blocking neutrophil recruitment. *J Pharmacol Exp Ther* 322:923–930.
11. Sasaki T, et al. (2000) Function of PI3Kgamma in thymocyte development, T cell activation, and neutrophil migration. *Science* 287:1040–1046.
12. Dimitratos SD, Woods DF, Stathakis DG, Bryant PJ (1999) Signaling pathways are focused at specialized regions of the plasma membrane by scaffolding proteins of the MAGUK family. *Bioessays* 21:912–921.
13. Anderson JM (1996) Cell signalling: MAGUK magic. *Curr Biol* 6:382–384.
14. Chishti AH (1998) Function of p55 and its nonerythroid homologues. *Current Opinion in Hematology* 5:116–121.
15. Marfatia SM, Lue RA, Branton D, Chishti AH (1994) In vitro binding studies suggest a membrane-associated complex between erythroid p55, protein 4.1, and glycophorin C. *J Biol Chem* 269:8631–8634.
16. Kim AC, Metzenberg AB, Sahr KE, Marfatia SM, Chishti AH (1996) Complete genomic organization of the human erythroid p55 gene (MPP1), a membrane-associated guanylate kinase homologue. *Genomics* 31:223–229.
17. Peters LL, Kirley LA, Kim AC, Chishti AH (1996) Localization of the gene encoding the erythrocyte membrane protein p55 (Mpp1) on the mouse X Chromosome. *Mammalian Genome* 7:245–246.
18. Ruff P, Speicher DW, Chishti A (1991) Molecular identification of a major palmitoylated erythrocyte membrane protein containing the src homology 3 motif. *Proc Natl Acad Sci USA* 88:6595–6599.
19. Metzenberg AB, Gitschier J (1992) The gene encoding the palmitoylated erythrocyte membrane protein, p55, originates at the CpG island 3′ to the factor VIII gene. *Hum Mol Genet* 1:97–101.
20. Hassock S, Vetrie D, Giannelli F (1999) Mapping and characterization of the X-linked dyskeratosis congenita (DKC) gene. *Genomics* 55:21–27.
21. Dokal I, Vulliamy T (2003) Dyskeratosis congenita: Its link to telomerase and aplastic anaemia. *Blood Rev* 17:217–225.
22. Ruggero D, et al. (2003) Dyskeratosis congenita and cancer in mice deficient in ribosomal RNA modification. *Science* 299:259–262.
23. Seo PS, et al. (2009) Identification of erythrocyte p55/MPP1 as a binding partner of NF2 tumor suppressor protein/Merlin. *Exp Biol Med (Maywood)* 234:255–262.
24. Benard V, Bohl BP, Bokoch GM (1999) Characterization of Rac and Cdc42 activation in chemoattractant-stimulated human neutrophils using a novel assay for active GTPases. *J Biol Chem* 274:13198–13204.
25. Alloisio N, et al. (1993) Evidence that red blood cell protein p55 may participate in the skeleton-membrane linkage that involves protein 4.1 and glycophorin C. *Blood* 82:1323–1327.
26. Siegrist SE, Doe CQ (2005) Microtubule-induced Pins/Galphai cortical polarity in Drosophila neuroblasts. *Cell* 123:1323–1335.
27. Mburu P, et al. (2006) Whirlin complexes with p55 at the stereocilia tip during hair cell development. *Proc Natl Acad Sci USA* 103:10973–10978.
28. Gosens I, et al. (2007) MPP1 links the Usher protein network and the Crumbs protein complex in the retina. *Hum Mol Genet* 16:1993–2003.
29. Elder B, et al. (1996) cDNA sequence and genomic structure of the murine p55 (Mpp1) gene. *Genomics* 38:231–234.
30. Southgate CD, Chishti AH, Mitchell B, Yi SJ, Palek J (1996) Targeted disruption of the murine erythroid band 3 gene results in spherocytosis and severe haemolytic anaemia despite a normal membrane skeleton. *Nat Genet* 14:227–230.